

# Trajectory-based Statistical Forwarding for Multi-hop Infrastructure-to-Vehicle Data Delivery

Jaehoon (Paul) Jeong, *Member, IEEE*, Shuo Guo, *Student Member, IEEE*, Yu (Jason) Gu, *Member, IEEE*, Tian He, *Member, IEEE*, and David H.C. Du, *Fellow, IEEE*

**Abstract**—This paper proposes Trajectory-based Statistical Forwarding (TSF) scheme, tailored for the multi-hop data delivery from infrastructure nodes (e.g., Internet access points) to moving vehicles in vehicular ad-hoc networks. To our knowledge, this paper presents the first attempt to investigate how to effectively utilize the packet destination vehicle's trajectory for such an infrastructure-to-vehicle data delivery. This data delivery is performed through the computation of a target point based on the destination vehicle's trajectory that is an optimal rendezvous point of the packet and the destination vehicle. TSF forwards packets over multi-hop to a selected target point where the vehicle is expected to pass by. Such a target point is selected optimally to minimize the packet delivery delay while satisfying the required packet delivery probability. The optimality is achieved analytically by utilizing the packet's delivery delay distribution and the destination vehicle's travel delay distribution. Through theoretical analysis and extensive simulation, it is shown that our design provides an efficient data forwarding under a variety of vehicular traffic conditions.

**Index Terms**—Vehicular Network, Road Network, Infrastructure, I2V, Data Forwarding, Trajectory, Delivery Delay, Delivery Probability.

## 1 INTRODUCTION

Vehicular Ad Hoc Networks (VANETs) have recently emerged as one of promising research areas for the driving safety in road networks [1]–[7]. As a result, the IEEE standards association has been working for wireless access in vehicular environments, standardizing Dedicated Short Range Communications (DSRC), such as IEEE 802.11p [8]. In the meantime, the GPS technology has been adopted for navigation purposes at an unprecedented rate. It is expected that approximately 300 million GPS devices will be shipped in 2009 alone [9]. It seems a very timely topic to develop the vehicular networking by integrating the cutting-edge DSRC and GPS technologies. Especially, our work is inspired by this current trend that a huge number of vehicles have started to install GPS-receivers for navigation and are considering DSRC devices for driving safety. The drivers are guided by these GPS-based navigation systems to select better driving paths in terms of the physically shortest path or the vehicular low-density traffic path. Therefore, one natural

research question is how to make the most of these GPS-guided driving paths to improve the performance of vehicular networks.

Let's consider the scenario (i) where a Traffic Control Center [10], [11] collects road network condition and maintains the trajectories of vehicles to want such up-to-date condition and (ii) where Access Points (APs) [12], [13] sparsely deployed in road networks are interconnected with each other along with the Traffic Control Center. These APs are used to provide individual vehicles with customized driving path information, such as driving hazards (e.g., holes, bumps, and slippery spots), accidents, and congested areas. With the customized driving path information, each individual vehicle can select another roadway (or lane) to escape from the possible dangerous situations for the driving safety or compute another travel path to lead to the more efficient driving for the further congested areas.

This individually customized driving path information needs to be delivered from the Traffic Control Center to each packet destination vehicle via APs. Rather than the broadcast data delivery approach of road network condition, the unicast data delivery approach is preferred in terms of data traffic volume. This is because vehicles have different trajectories and so they do need the driving path information only along their trajectory. Since the APs have the limited communication coverage, the infrastructure-to-vehicle data delivery can be supported using vehicular ad-hoc networks to bridge the APs and the packet destination vehicles. However, due to the dynamic mobility in the road networks, the Disruption Tolerant Networking (DTN) is required for data delivery in vehicular networks [14]. For vehicular DTN, state-of-the-art schemes [3], [15]–[18] have adopted the *carry-and-forward* approach and have demonstrated their effectiveness in the data forwarding from a moving source (e.g., vehicle) to a stationary destination (e.g., AP). However, these schemes are not designed for the infrastructure-to-vehicle data delivery (called reverse data forwarding). This reverse data forwarding is more challenging because the packet destination is moving during the packet delivery. For this forwarding, the packet destination position needs to be accurately estimated considering the temporal-and-spatial rendezvous of the packet and the destination vehicle.

To the best of our knowledge, our Trajectory-based Statistical Forwarding (TSF) is the first work to investigate

• J. (Paul) Jeong, S. Guo, Y. (Jason) Gu, T. He, and D.H.C. Du are with the Department of Computer Science and Engineering, University of Minnesota, Twin Cities, 200 Union Street SE, Minneapolis, MN 55455.  
E-mail: {jjeong,sguo,yugu,tianhe,du}@cs.umn.edu.

the reverse data forwarding based on the vehicle trajectory guided by GPS-based navigation systems [19] for the efficient-and-safe driving. To ensure the rendezvous of a packet and a destination vehicle, an optimal target point is identified as a packet destination position in the road network in order to minimize the packet delivery delay while satisfying the user-required packet delivery probability. In order to search such an optimal target point, our key idea is to use the two delay distributions: (i) the packet delivery delay distribution from the AP to the target point and (ii) the vehicle travel delay distribution from the destination vehicle's current position to the target point. Once the target point is decided, our TSF adopts the source routing technique, i.e., forwards the packet toward the target point by using the shortest-delay forwarding path specified by multiple intersections in the target road network. Our intellectual contributions are as follows:

- An infrastructure-to-vehicle data delivery architecture,
- The delay modeling for packet and vehicle, and
- An optimal target point selection algorithm.

The rest of this paper is organized as follows: First of all, we summarize related work for vehicular networking in Section 2. In Section 3, we then formulate our infrastructure-to-vehicle data delivery problem with the relay-node-based forwarding architecture. Section 4 explains our optimal target point selection. Section 5 explains the packet delay model and the vehicle delay model for target point computation. Section 6 explains the TSF forwarding protocol. Section 7 evaluates our design. We finally conclude this paper along with future work in Section 8.

## 2 RELATED WORK

Recently, the VANET research has put a lot of attention on the data forwarding and data dissemination for vehicle-to-vehicle or vehicle-to-infrastructure communications [1], [3]–[7], [20], [21]. The data forwarding in VANET is different from that in the traditional mobile ad-hoc networks (MANETs) [22] for the reasons of (i) vehicles are moving on the physically constrained areas (i.e., roadways), (ii) the moving speed of vehicles is also constrained by the speed limit on the roadways, and (iii) the communication shortest paths do not always match the physical shortest paths due to heterogeneous traffic conditions on road segments. These unique characteristics of the road networks open the new door of research opportunities for the data forwarding in the VANET. Also, the frequent network partition and merge due to the high mobility of vehicles makes the MANET routing protocols [22] ineffective in the VANET settings [23]. Thus, in order to deal with such a frequent network partition and merge, the *carry-and-forward* approaches are required. Epidemic Routing [15] is an early work to handle this issue through the random pair-wise exchange of data packets among mobile nodes. However, it is designed for two-dimensional open fields, not optimized for the road networks with the confined routes for vehicles.

Data forwarding schemes investigating the layout of road network and vehicular traffic statistics are proposed in VADD [3], Delay-Bounded Routing [4], and SADV [17]. VADD

investigates the data forwarding using a stochastic model based on vehicular traffic statistics in order to achieve the *lowest delivery delay* from a mobile vehicle to a stationary packet destination, such as Access Point (AP). Delay-Bounded Routing proposes data forwarding schemes to satisfy the *user-defined delay bound* rather than the *lowest delivery delay*. In addition, it also aims at minimizing the channel utilization in terms of the number of packet transmissions. In SADV [17], authors also propose a forwarding strategy that leverages relay nodes in the network for the reliable data delivery. For all those existing approaches, they focus on the data forwarding from vehicles to a fixed destination (e.g., AP).

With increasingly popular usage of GPS devices, *vehicle trajectory information* has become a new valuable input for effective data forwarding schemes. Our earlier work TBD [16] utilizes such vehicle trajectory information along with vehicular traffic statistics to further improve communication delay and delivery probability for vehicle-to-static-destination communications. In TBD, the vehicle trajectory is used to compute a forwarding-decision-making metric called Expected Delivery Delay from the vehicle's current position to the packet destination. In this paper, we take a step further and provide an efficient solution for forwarding messages from a fixed destination (i.e., AP) to a mobile node (i.e., vehicle) by using the trajectory of the mobile destination. In TSF, the packet destination's vehicle trajectory is used to select an optimal rendezvous point of the packet and the destination vehicle.

Access Points are important for the infrastructure-to-vehicle communications. In [7], Bychkovsk et al. show the feasibility that vehicles can access open WiFi access points providing the wired network connections in vehicular networks. *Cabernet* [6] also proposes one-hop Internet access schemes using open WiFi access points in vehicular network. Their target is different from TSF's in that TSF considers the multi-hop data delivery from APs to vehicles. Recently, in [24], Banerjee et al. propose approaches to enhance mobile networks, such as vehicular networks, with infrastructure nodes, such as relays, base stations, and mesh nodes. However, their forwarding scheme is limited to *two-hop-distance* data forwarding; that is, a source vehicle forwards packets to a nearby infrastructure network node and then the infrastructure network forwards the packets to another infrastructure node close to the destination vehicle. On the other hand, our TSF can be extended to support the multi-hop vehicle-to-vehicle communications through the infrastructure nodes (i.e., APs and relay nodes). That is, for the multi-hop two-way communications between vehicles, the data delivery from source vehicle to AP can be performed by our early work TBD and the reverse data delivery from AP to destination vehicle can be performed by our TSF proposed in this paper.

## 3 PROBLEM FORMULATION

In this section, we formulate the data forwarding in vehicular networks as follows: *Given a road network with APs, our goal is to deliver packets reliably from the APs to a moving destination vehicle with a minimum End-to-End (E2E) delay.*

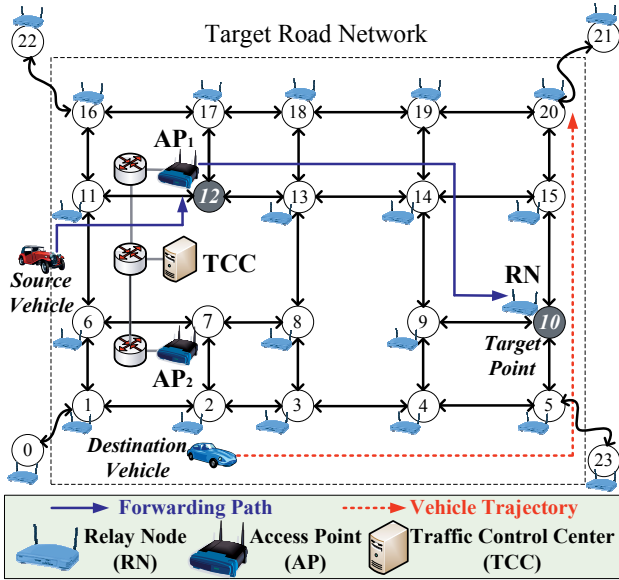


Fig. 1. Data Forwarding in Vehicular Networks

### 3.1 Assumptions

This work is based on the following set of assumptions on the road network and vehicle settings.

- Access Point (AP) is a wireless network node connected to the wired network (e.g., the Internet) with DSRC device, storage and processor in order to provide vehicles with the wired network connectivity. For the cost effectiveness, as shown in Fig. 1, APs are sparsely deployed into road networks and are interconnected with each other through the wired network or wirelessly (as Mesh Network) for the data forwarding. It is known that each AP installation with power and wired network connectivity can cost as high as US\$5,000 [25]. The geographical location information of APs is available to vehicles. A couple of studies have been done to utilize the APs available on the road-sides [6], [7].
- Traffic Control Center (TCC) is a trustable entity that maintains vehicle trajectories without exposing the vehicle trajectories to other vehicles for privacy concerns. We can integrate vehicular networks to the existing TCCs used for the road traffic engineering [10], [11]. As shown in Fig. 1, TCC and APs are interconnected with each other through the wired network, such as the Internet. TCC selects an AP among multiple APs as the first hop for the data delivery toward the destination vehicle in terms of the shortest delivery delay to the destination vehicle. Note that for simplicity, we do not denote TCC explicitly in the road network later in this paper.
- Relay Node (RN) is a temporary packet holder with DSRC device, storage and processor in vehicular ad-hoc networks that is a stand-alone node without the wired network connectivity to APs, as shown in Fig. 1. For the sake of clarity, RN is assumed to be deployed at each intersection. This deployment is required to support the reliable data delivery from infrastructure node (i.e., AP) to mobile node (i.e., vehicle), as explained in Section 3.2. We discuss the relaxation of this assumption in Section 6.4

that our data forwarding scheme works even in the case where some intersections do not have their own RNs.

- Vehicles participating in VANET have DSRC devices [8]. Nowadays many vehicle vendors, such as GM and Toyota, are planning to release vehicles with DSRC devices for the driving safety [13], [26].
- Vehicles, TCC, APs, and RNs are installed with GPS-based navigation systems and digital road maps [19], [27]. Traffic statistics, such as vehicle arrival rate  $\lambda$  and average vehicle speed  $v$  per road segment, are available via commercial navigation systems (e.g., Garmin [19]).
- Drivers input their travel destination into their GPS-based navigation systems before their travel and so their vehicles can compute their future trajectory based on their current location and their final destination. Vehicles regularly report their trajectory information and their current location to TCC via APs, using vehicle-to-infrastructure data forwarding schemes, such as VADD [3], TBD [16], and SADV [17]. These participant vehicles can be localized by TCC with their registered trajectories when an infrastructure node (i.e., AP) has data packets to send them.

TABLE 1  
 Delay Average Estimation of VADD

Protocol	Expected Delay	Actual Delay	Error
VADD	489.1sec	412.5sec	15.7%

TABLE 2  
 Delay Standard Deviation (STD) of VADD

Protocol	Expected STD	Actual STD	Error
VADD	10.1sec	139.2sec	1277.1%

### 3.2 Relay-Node-Assisted Forwarding

The data forwarding from vehicle to AP (i.e., fixed destination) has already been researched with *stochastic models*, such as VADD [3] and TBD [16]. These stochastic models try to forward packets opportunistically toward the packet destination using *in-situ next carriers* without relay nodes at intersections. For example, Fig. 1 shows the vehicle-to-infrastructure data forwarding from *Source Vehicle* to  $AP_1$  and for this data forwarding, we can use either VADD or TBD. Both VADD and TBD demonstrate the effectiveness of their approaches, mainly in the case where the final destination is a fixed access point. However, the data forwarding from the AP to the vehicle (called reverse data forwarding) is a completely different story, such as the forwarding from  $AP_1$  to *Destination Vehicle* in Fig. 1. The success ratio of this reverse data forwarding highly depends on the accuracy of delay estimation, because only *just-in-time* packets can be delivered to a moving vehicle.

To investigate whether we can apply existing infrastructure-free forwarding technique such as VADD [3], we conduct simulations in the road network. As shown in Fig. 1,  $AP_1$  is placed at intersection  $n_{12}$  and the target point is intersection  $n_{10}$ .  $AP_1$  at  $n_{12}$  generates 5000 packets with the exponential distribution of 1-second interval toward the relay node (denoted as  $RN$ ) at

the target point  $n_{10}$ . As shown in the figure, one of possible packet forwarding paths is  $n_{12} \rightarrow n_{13} \rightarrow n_{14} \rightarrow n_9 \rightarrow n_{10}$ .

Table 1 and Table 2 show the statistics of VADD's packet delivery delay from the AP at  $n_{12}$  (denoted as  $AP_1$ ) to the relay node at the target point  $n_{10}$  (denoted as  $RN$ ). Clearly, from Table 1, it can be seen that VADD has a very large delay estimation error in that the mean of the expected delivery delay is much different from that of the actual delivery delay. More noticeably, from Table 2, VADD has a standard deviation (STD) estimation error of 1277.1%, a value that makes just-in-time delivery difficult, if not possible. Such a large uncertainty is introduced by the stochastic forwarding at the intersection, where a vehicle might carry the packet along a wrong direction if no vehicle at the intersection moves toward the right direction. In the rest of the paper, we demonstrate such a large uncertainty should and can be reduced by deploying relay nodes at the intersections. Note that SADV [17] is an early work to investigate the relay-node-assisted forwarding in vehicular networks, however, it does not consider the reverse forwarding from APs to moving vehicles.

### 3.3 Concept of Operation in TSF

Fig. 1 shows the data packet forwarding from an AP to a destination vehicle. Suppose that as shown in the figure, the destination vehicle has its vehicle trajectory consisting of 7 intersections, that is,  $n_2 \rightarrow n_3 \rightarrow \dots \rightarrow n_{20}$  and has registered its vehicle trajectory into the Traffic Control Center via APs. Our goal is to deliver packets from the AP to the destination vehicle with a short delay. As shown in Fig. 1, our delivery strategy is to let the packets arrive earlier at a target point (i.e., intersection  $n_{10}$  on the destination vehicle's trajectory) along the forwarding path for the target point than the destination vehicle. Since there exists a relay node at the target point, the packets earlier arrived can wait for the destination vehicle. Thus, this target point is determined as a *rendezvous point* where the packet is highly expected to meet the destination vehicle with the shortest packet delay.

For the driving guidance services in vehicular networks, the data upload and download should be considered together for sharing road safety information among vehicles via APs. For the upload of road safety information collected by vehicles as well as the download, we can use (i) our TSF by regarding APs as packet destinations or (ii) the existing data forwarding schemes (e.g., VADD [3] and TBD [16]) for the vehicle-to-infrastructure data delivery. This indicates that our TSF can support the vehicle-to-vehicle data delivery via APs, that is, the data delivery from *Source Vehicle* to *Destination Vehicle* via  $AP_1$  in Fig. 1. In the next section, we will explain how to determine an optimal target point on the vehicle trajectory.

## 4 TARGET POINT SELECTION FOR DATA DELIVERY

In this section, we explain how to select an optimal target point for the data delivery from an AP to a destination vehicle with the packet delay and vehicle delay distributions. The target point selection is based on the *delivery probability* that the

packet will arrive earlier than the destination vehicle at the target point. This delivery probability can be computed with the packet's delivery delay distribution and the destination vehicle's travel delay distribution as follows. Let  $I$  be the set of intersections consisting of the destination vehicle's trajectory. Let  $i$  be a target point where  $i \in I$ . Let  $\alpha$  be the user-required delivery probability. Let  $P_i$  be the packet delay that a packet will be delivered from AP to target point  $i$ . Let  $V_i$  be the vehicle delay that the destination vehicle will move from its current position to target point  $i$ . For example, in Fig. 1,  $P_{10}$  is the expected packet delay that a packet will be delivered from AP to target point  $n_{10}$  and  $V_{10}$  is the expected vehicle delay that Destination Vehicle will move from its current position  $n_2$  to target point  $n_{10}$ . Thus, we can compute the delivery probability as  $P[P_i \leq V_i]$ .

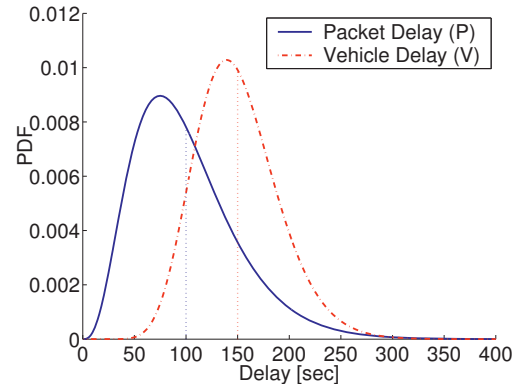


Fig. 2. Packet Delay Distribution and Vehicle Delay Distribution

Given a user-required delivery probability threshold  $\alpha$ , we select a target point intersection  $i$  with the minimum vehicle movement delay as an optimal target point such that  $P[P_i \leq V_i] \geq \alpha$ . Note that the minimum vehicle movement delay determines the destination vehicle's packet reception delay. More formally, we can select an optimal target point with a minimum delivery delay while satisfying the delivery probability  $\alpha$  as follows:

$$i^* \leftarrow \arg \min_{i \in I} E[V_i] \quad \text{subject to } P[P_i \leq V_i] \geq \alpha. \quad (1)$$

In (1), the delivery probability  $P[P_i \leq V_i]$  is the probability that the packet will arrive earlier at target point  $i$  than the destination vehicle. Fig. 2 shows the distribution of packet delay  $P$  and the distribution of vehicle delay  $V$ .

We model the distributions of packet delay and vehicle delay as the Gamma distributions such that  $P \sim \Gamma(\kappa_p, \theta_p)$  and  $V \sim \Gamma(\kappa_v, \theta_v)$  [28]. We will describe this delay modeling in detail in Section 5. Note that our delay models are not restricted to the Gamma distributions and can accommodate any empirical distributions. That is, if more accurate distributions are available, our model can use them for the computation of the delivery probability. Given that the packet delay distribution and the vehicle delay distribution are independent of each other, the delivery probability  $P[P_i \leq V_i]$  is computed as follows:

$$P[P_i \leq V_i] = \int_0^{TTL} \int_0^v f(p)g(v)dpdv. \quad (2)$$

where  $f(p)$  is the probability density function (PDF) of packet delay  $p$ ,  $g(v)$  is the PDF of vehicle delay  $v$ , and  $TTL$  is the packet's Time-To-Live (TTL); TTL is determined as the destination vehicle trajectory's lifetime that is the destination vehicle's travel time from its current position to its last position on the trajectory. Note that the delivery probability is computed considering the packet's lifetime  $TTL$ ; that is, since the packet is discarded after  $TTL$ , the probability portion is zero after  $TTL$ . Clearly, the optimal target point selection depends on the packet delay model  $P$  and the vehicle delay model  $V$  which are described in the next section.

## 5 DELAY MODELS

In this section, we describe two types of delay models: (i) Packet delay model and (ii) Vehicle delay model. For the packet delay model, we first describe the link delay taken for the packet to be delivered over a road segment in Section 5.1 and then the E2E packet delay distribution from one position to another position on the road network in Section 5.2. For the vehicle delay model, we explain how to construct the vehicle delay distribution from the vehicle's current position to a target point in Section 5.3.

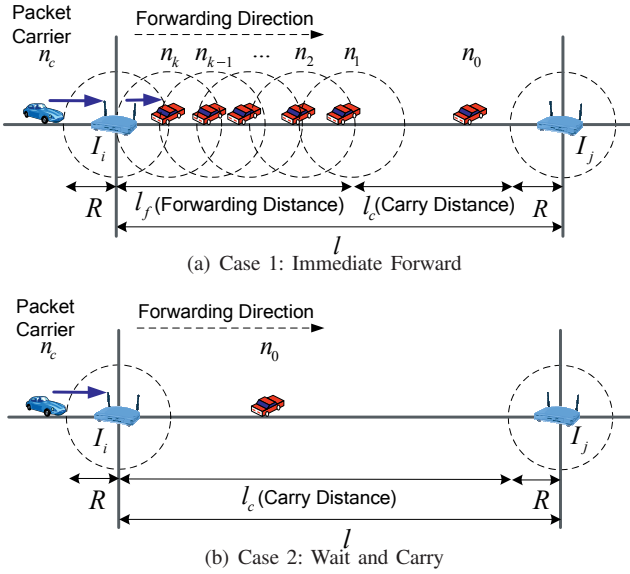


Fig. 3. Link Delay Modeling for Road Segment

### 5.1 Link Delay Model

This subsection analyzes the link delay for one road segment with one-way road traffic given the vehicle inter-arrival time, the vehicle speed, and the communication range. It is supposed that one relay node for packet buffering is placed at each end-point (i.e., intersection) of the road segment, as shown in Fig. 3. In this paper, for the simplified mathematical analysis of link delay, we focus on the link delay model in one-way road traffic. The link delay model in two-way road traffic will be investigated as future work, which can easily be integrated into our TSF design.

Also, it should be noted that in the VANET scenarios, the carry delay is *several orders-of-magnitude* longer than the

communication delay. For example, a vehicle takes 90 seconds to travel along a road segment of 1 mile with a speed of 40 MPH, however, it takes *only ten of milliseconds* to forward a packet over the same road segment, even after considering the retransmission due to wireless link noise or packet collision; this short retransmission time is because the data rate in DSRC [8] is 6~27 Mbps and transmission range can extend to almost 1,000 meters. Thus, since the carry delay is the dominating part of the total delivery delay, in our analytical model for the link delay we focus on the carry delay for the sake of clarity, although the small communication delay does exist in our design.

The link delay for one road segment can be computed by considering the following two cases for the communication range of the relay node at intersection  $I_i$  in Fig. 3:

- **Case 1: Immediate Forward:** There is at least one vehicle (i.e.,  $k > 0$ ) moving toward the intended next intersection along the packet's forwarding path. The current *packet carrier*  $n_c$  forwards its packets to the relay node at intersection  $I_i$ . As shown in Fig. 3(a), the relay node forwards the packets to vehicle  $n_k$  right away and the packets are forwarded up to vehicle  $n_1$ , that is, by the forwarding distance  $l_f$ , which is the length of the connected ad-hoc network consisting of vehicles  $n_i$  for  $i = 1..k$ . Vehicle  $n_1$  will carry the packets up to the communication range of the relay node at  $I_j$ , that is, by the carry distance  $l_c$ . Note that the link delay for this case is analyzed in our previous work called *TBD* [16].
- **Case 2: Wait and Carry:** There is no vehicle (i.e.,  $k = 0$ ) moving toward the intended next intersection along the packet's forwarding path. As shown in Fig. 3(b), the current *packet carrier*  $n_c$  forwards its packets to the relay node at intersection  $I_i$ . The relay node stores the packets at its local storage as a packet holder until a vehicle moves on the road segment  $(I_i, I_j)$ . The average waiting time is  $1/\lambda$  where the vehicle arrival rate is  $\lambda$  on the road segment  $(I_i, I_j)$ ; note that we will explain how to obtain  $\lambda$  later. After this average waiting, the new packet carrier will carry the packets by the carry distance  $l_c (= l - R)$ .

Thus, we can compute the expectation of the link delay with the link delays of these two cases as follows:

$$d = \begin{cases} \frac{l - l_f - R}{v} & \text{for case 1: immediate forward,} \\ \frac{1}{\lambda} + \frac{l - R}{v} & \text{for case 2: wait and carry.} \end{cases} \quad (3)$$

$$\begin{aligned} E[d] &= E[\text{link delay} \mid \text{forward}] \times P[\text{forward}] \\ &\quad + E[\text{link delay} \mid \text{wait}] \times P[\text{wait}] \\ &= \frac{l - R - E[l_f]}{v} \beta + \left( \frac{1}{\lambda} + \frac{l - R}{v} \right) (1 - \beta) \end{aligned} \quad (4)$$

where  $P[\text{forward}] = \beta = 1 - e^{-\frac{\lambda R}{v}}$  and  $P[\text{wait}] = 1 - \beta = e^{-\frac{\lambda R}{v}}$ ; note that we will explain how to compute  $\lambda$  and  $\beta$  later. Please, refer to Appendix A.1 for the detailed derivation of  $E[d]$ . Also, in the similar way, we can compute the variance

of the link delay as follows:

$$\begin{aligned} Var[d] &= E[d^2] - (E[d])^2 \\ &= \frac{(l-R)^2 - 2(l-R)E[l_f] + E[l_f^2]}{v^2} \beta \\ &\quad + \left(\frac{1}{\lambda} + \frac{l-R}{v}\right)^2 (1-\beta) \\ &\quad - \left(\frac{l-R-E[l_f]}{v}\right) \beta + \left(\frac{1}{\lambda} + \frac{l-R}{v}\right) (1-\beta)^2. \end{aligned} \quad (5)$$

Please, refer to Appendix A.2 for the detailed derivation.

Now we explain how to obtain the vehicle arrival rate  $\lambda$  and the forwarding probability  $\beta$  per road segment. First, the vehicle arrival rate  $\lambda$  can be obtained with Fig. 3 as follows: Whenever a vehicle passes through the intersection  $I_i$  toward the neighboring intersection  $I_j$ , it reports its passing timestamp for the relay node at  $I_i$ . With a series of reported passing timestamps for the road segment  $(I_i, I_j)$ , the relay node at the entrance intersection  $I_i$  can compute  $\lambda$  for the outgoing edge  $(I_i, I_j)$  by averaging the sum of the vehicle interarrival times and taking the reciprocal of the average. In the same way, the relay node at the exit intersection  $I_j$  can compute the arrival rate  $\lambda$  for the incoming edge  $(I_i, I_j)$  with the passing timestamps for  $I_j$ . Second, the forwarding probability  $\beta$  can be computed with Fig. 3 as follows: Let  $T$  be the passing time from the intersection of a relay node to the communication range  $R$  of the relay node. When the vehicle speed is  $v$ , the passing time is computed as  $T = R/v$ . Suppose that the vehicle arrival at the directed edge  $(I_i, I_j)$  is Poisson process with vehicle arrival rate  $\lambda$ . The probability that at least one vehicle arrives at the entrance intersection  $I_i$  for the duration  $T$  means the forwarding probability. Thus, from the Poisson process probability [28] that the arrival number  $N$  is at least one (i.e.,  $N > 0$ ) for the unit time, the forwarding probability  $\beta$  can be computed as follows:

$$P[\text{forward}] = P[N > 0] = \beta = 1 - e^{-\lambda T} = 1 - e^{-\frac{\lambda R}{v}}. \quad (6)$$

Finally, with the mean  $E[d]$  in (4) and variance  $Var[d]$  in (5) of the link delay, we model the link delay  $d$  as the Gamma distribution. Note that the Gamma distribution is usually used to model the positive continuous random variable, such as the waiting time and lifetime [28]. Based on the Gamma distribution, a simplified mathematical model is used in this paper to obtain the packet's link delay distribution over a road segment, however, our design can accommodate an empirical link delay distribution if available through measurement. For this empirical distribution of link delay, adjacent relay nodes can periodically exchange probe packets with each other to obtain link delay samples. These samples are periodically processed by the relay nodes, which report the link delay statistics to TCC. Thus, the distribution of the link delay  $d_i$  for the edge  $e_i \in E[G]$  is  $d_i \sim \Gamma(\kappa_i, \theta_i)$  such that  $E[d_i] = \kappa_i \theta_i$  and  $Var[d_i] = \kappa_i \theta_i^2$  for  $d_i, \kappa_i, \theta_i > 0$  [28]. Since we have the mean and variance of the link delay, that is,  $E[d_i] = \mu_i$  in (4) and  $Var[d_i] = \sigma_i^2$  in (5), we can compute the parameters  $\theta_i$  and  $\kappa_i$  of the Gamma distribution as follows:

$$\theta_i = \frac{Var[d_i]}{E[d_i]} = \frac{\sigma_i^2}{\mu_i}. \quad (7)$$

In (7), the parameter  $\theta_i$  is computed by dividing the link delay variance by the mean link delay.

$$\kappa_i = \frac{E[d_i]}{\theta_i} = \frac{\mu_i}{\theta_i} = \frac{\mu_i^2}{\sigma_i^2}. \quad (8)$$

In (8), the parameter  $\kappa_i$  is computed by dividing the mean link delay by the parameter  $\theta_i$  in (7).

Up to now, we have modeled the link delay for a directed edge corresponding to a road segment. Next, with the distribution of the link delay for each edge, we can compute the E2E packet delay from the AP to the target point, assuming the independence of the link delays for the road segments consisting of the E2E forwarding path from the AP to the target point. In the next section, we will construct the distribution of the packet delay from the AP to a target point as the Gamma distribution.

## 5.2 E2E Packet Delay Model

In this subsection, we model the End-to-End Packet Delay from one position to another position in a given road network. As discussed in Section 5.1, the link delay is modeled as the Gamma distribution of  $d_i \sim \Gamma(\kappa_i, \theta_i)$  for edge  $e_i \in E(G)$  in the road network graph  $G$ . Given a forwarding path from AP to a target point, we assume that the link delays of edges consisting of the path are independent. From this assumption, the mean and variance of the E2E packet delay are computed as the sum of the means and the sum of the variances of the link delays along the E2E path, respectively. Assuming that the forwarding path consists of  $N$  edges, the mean and variance of the E2E packet delay distribution can be computed as follows:

$$E[P] = \sum_{i=1}^N E[d_i] = \sum_{i=1}^N \mu_i. \quad (9)$$

$$Var[P] = \sum_{i=1}^N Var[d_i] = \sum_{i=1}^N \sigma_i^2. \quad (10)$$

With (9) and (10), the E2E packet delay distribution can be modeled as  $P \sim \Gamma(\kappa_p, \theta_p)$  such that  $E[P] = \kappa_p \theta_p$  and  $Var[P] = \kappa_p \theta_p^2$  for  $P, \kappa_p, \theta_p > 0$  [28].

## 5.3 Vehicle Delay Model

In this subsection, we model the Vehicle Delay from one position to another position in a given road network. Given the road network graph  $G$ , the travel time for edge  $e_i \in E(G)$  is modeled as the Gamma distribution of  $t_i \sim \Gamma(\kappa_i, \theta_i)$ ; note that the travel time distribution for each road segment can be obtained through vehicular traffic measurement and is usually considered the Gamma distribution [29], [30]. The parameters  $\kappa_i$  and  $\theta_i$  of the Gamma distribution are computed with the mean travel time  $\mu_i$  and the travel time variance  $\sigma_i^2$  using the relationship among the mean  $E[t_i]$ , the variance  $Var[t_i]$ ,  $\kappa_i$ , and  $\theta_i$  such that  $E[t_i] = \kappa_i \theta_i$  and  $Var[t_i] = \kappa_i \theta_i^2$  for  $t_i, \kappa_i, \theta_i > 0$  [28] as follows:

$$\theta_i = \frac{Var[t_i]}{E[t_i]} = \frac{\sigma_i^2}{\mu_i}. \quad (11)$$

In (11), the parameter  $\theta_i$  is computed by dividing the travel time variance by the mean travel time.

$$\kappa_i = \frac{E[t_i]}{\theta_i} = \frac{\mu_i}{\theta_i} = \frac{\mu_i^2}{\sigma_i^2}. \quad (12)$$

In (12), the parameter  $\kappa_i$  is computed by dividing the mean travel time by the parameter  $\theta_i$  in (11).

Given a vehicle trajectory from the vehicle's current position to a target point, we suppose that the travel times of edges consisting of the trajectory are independent. Especially, this assumption is valid in light-traffic vehicular networks where vehicles are a little affected by other vehicles in their travel. We leave the End-to-End travel delay modeling in heavy-traffic vehicular networks as future work. Note that the model for the heavy traffic can easily be plugged into our TSF design if available. Assuming that the trajectory consists of  $N$  edges, in the same way with the Packet Delay Model in Section 5.2, the mean  $E[V]$  and variance  $Var[V]$  of the E2E vehicle delay can be computed such that  $E[V] = \sum_{i=1}^N \mu_i$  and  $Var[V] = \sum_{i=1}^N \sigma_i^2$ . Therefore, the E2E vehicle delay distribution can be modeled as  $V \sim \Gamma(\kappa_v, \theta_v)$  such that  $E[V] = \kappa_v \theta_v$  and  $Var[V] = \kappa_v \theta_v^2$  for  $V, \kappa_v, \theta_v > 0$  [28].

So far we have modeled the packet delay and the vehicle delay. Our design depends on the accuracy of the packet delay distribution and the vehicle delay distribution. In this paper, we approximated those delay distributions as the Gamma distributions, but this approximation may not work well in some realistic scenarios, such as heavy-traffic or congested vehicular networks. However, even in these challenging scenarios, if the delay distributions can be available through measurements, our design can still work by performing the correct target point selection. In the next section, based on our TSF design and delay models, we will explain our forwarding protocol considering the scenarios with multiple APs.

## 6 TSF PROTOCOL

In this section, we explain the protocol of our Trajectory-based Statistical Forwarding (TSF).

### 6.1 Forwarding Protocol

In this subsection, we describe our design of TSF forwarding protocol for the infrastructure-to-vehicle data delivery in the given road network.

For the TSF forwarding protocol, the TSF packet format contains two important fields: (i) Forwarding Path and (ii) Vehicle Trajectory. *Forwarding Path* is the list of the intersections for the source routing from AP to the target point. *Vehicle Trajectory* is the destination vehicle's trajectory, that is, the series of intersections on the destination vehicle's trajectory. With this TSF packet format, the data packets will be forwarded toward the destination vehicle.

First of all, the destination vehicle periodically reports its future trajectory and current position to Traffic Control Center (TCC) in order to receive data packets from APs through TCC, discussed in Section 3. With this vehicle trajectory registered into TCC, TSF will forward the data packets from AP to the

destination vehicle by the following two steps: (i) The First-Step Forwarding from AP to Target Point (in Section 6.1.1) and (ii) The Second-Step Forwarding from Target Point to Destination Vehicle (in Section 6.1.2).

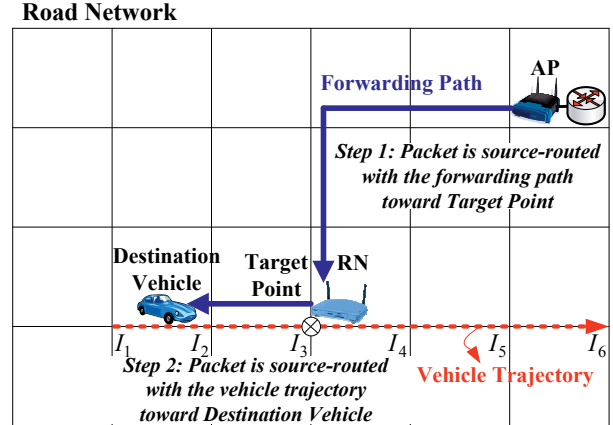


Fig. 4. TSF Forwarding Protocol

#### 6.1.1 The First-Step Forwarding from AP to Target Point

The first-step forwarding is to forward a packet through the source routing along the forwarding path from AP to the target point. When TCC has data packets to forward a destination vehicle, it computes the forwarding path for an optimal target point at the transmission time and forwards the data packets to an appropriate AP as the first hop. This first-hop AP will try to forward the packets to a vehicle moving along the forwarding path when the vehicle comes into the communication range of the AP. As shown in Fig. 4, the forwarding path is the *shortest packet delay path* from AP to the target point  $I_3$  determined by TCC with the optimization in (1). For example, as shown in Fig. 1, the forwarding path is  $n_{12} \rightarrow n_{13} \rightarrow n_{14} \rightarrow n_9 \rightarrow n_{10}$ . The relay nodes on the forwarding path are trying to forward the packets to carriers moving toward their neighboring relay nodes along the forwarding path.

During the forwarding process, it should be noted that only one packet copy exists in the vehicular network because TSF is a unicast data forwarding scheme. Thus, the current packet holder (i.e., AP, relay node, or current carrier) deletes its packet copy after forwarding the packet to the next hop (i.e., next carrier, relay node, or destination vehicle). In Fig. 1, the AP at  $n_{12}$  will try to forward the packets to a vehicle moving toward the neighboring relay node at  $n_{13}$  on the forwarding path. The intermediate relay nodes at  $n_{13}$ ,  $n_{14}$ , and  $n_9$  will try to forward the packets to their neighboring relay node along the forwarding path. In this way, the packet will be delivered to the relay node corresponding to the target point  $n_{10}$  in Fig. 1.

#### 6.1.2 The Second-Step Forwarding from Target Point to Destination Vehicle

The second-step forwarding is to forward a packet through the source routing along the reverse path of the vehicle trajectory from the target point toward the destination vehicle.

As shown in Fig. 4, when the packet arrives at the relay node corresponding to the target point  $I_3$ , the relay node will hold

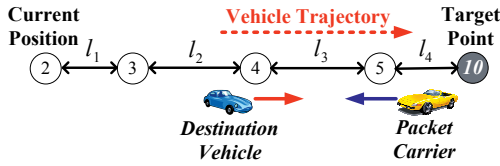


Fig. 5. Reverse Path Forwarding for Vehicle Trajectory

the packet until a vehicle passes it. If a vehicle is heading for the next intersection  $I_2$  on the reverse path of  $I_3 \rightarrow I_2 \rightarrow I_1$ , the relay node at  $I_3$  will forward its packet to the vehicle.

For example, in Fig. 5, if the relay node corresponding to the target point  $n_{10}$  finds a vehicle moving reversely on the destination vehicle’s trajectory (i.e., on  $n_{10} \rightarrow n_5$ ), it will forward its packet to the vehicle as next carrier. Note that the packet copy at the relay node is deleted after it is forwarded to the next carrier. The current carrier carries and forwards the packet to the next carrier moving toward the destination vehicle. As a reminder, when the packet is received by the next carrier, the packet copy at the current carrier is deleted. If the carrier goes out of the vehicle trajectory at  $n_5$  in Fig. 5 and there is not any other vehicle moving toward the destination, it forwards its packet to the relay node at  $n_5$  on the vehicle trajectory before its leaving from the vehicle trajectory. The relay node at  $n_5$  that takes over the packet will try to forward the packet to another carrier moving toward the destination vehicle along the reverse path of the vehicle trajectory. This process is repeated until the packet can be delivered to the destination vehicle.

The rationale of the reverse-path forwarding is that the optimization for a target point in (1) provides an optimal target point with the minimum packet delivery delay while satisfying the required delivery probability. This indicates that the packet will hit the destination vehicle along the destination vehicle’s trajectory if the packet follows the reverse path of the vehicle trajectory. Of course, there is some probability that the packet arrives at the target point later than the destination vehicle. In this case, the packet will not hit the destination vehicle, so will be discarded after its TTL expiration. In the performance evaluation in Section 7, we will show the delivery delay and the delivery ratio according to the user-required delivery probability threshold  $\alpha$ .

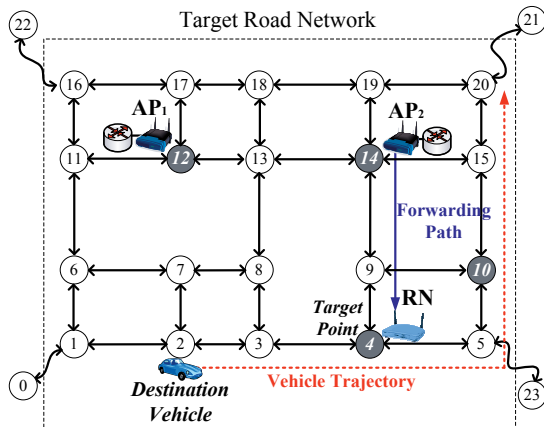


Fig. 6. Data Forwarding with Multiple APs

## 6.2 Data Forwarding with Multiple APs

In a large-scale road network, multiple Access Points (APs) are usually required to accommodate the infrastructure-to-vehicle data delivery. In this case, an AP with the minimum delivery delay can send the packets to a destination vehicle among the multiple APs; note that the multiple APs are interconnected with each other via the wired network (e.g., the Internet), so the communication delay among the APs are negligible compared with the carry delay at the second level. Also, note that the multiple APs share the estimated link delays of road segments (discussed in Section 5.1) to compute the E2E packet delay from their position to a target point. We can easily extend our data forwarding framework for this multiple-AP road network as follows. We determine the *Expected Vehicle Delay (EVD)* of the destination vehicle for the multiple APs as the minimum among the EVDs for the APs as follows:

$$EVD^* \leftarrow \min_{k \in AP} EVD_k \quad (13)$$

where  $AP$  is the set of APs and  $EVD_k$  is the EVD of the destination vehicle for access point  $AP_k$ ; note that the AP with the minimum EVD will try to send packets to the destination vehicle. For example, Fig. 6 shows the road network graph with two access points  $AP_1$  and  $AP_2$ . The  $EVD^*$  is  $\min \{EVD_1, EVD_2\}$  where  $EVD_1$  and  $EVD_2$  can be computed using (1) to satisfy the required delivery probability  $\alpha$ , respectively. In this figure, as a target point,  $AP_1$  and  $AP_2$  select  $n_{10}$  and  $n_4$ , respectively. Thus, the packet from  $AP_1$  to  $n_{10}$  can be received after  $EVD_1$  and the packet from  $AP_2$  to  $n_4$  can be received after  $EVD_2$ . Since  $EVD_2 < EVD_1$ , only  $AP_2$  will send the packet toward its target point  $n_4$ .

Note that APs can be interconnected via wireless links as Mesh Networks. In this case, the road segments within the coverage of these APs have no carry delay. That is, the link delay of these road segments can be considered zero. Even for this setting, our TSF protocol can still be used by adjusting the link delays in the road network graph.

In a large-scale road network, one Traffic Control Center (TCC) might not scale up to provide a large number of vehicles with the reverse data forwarding. For this system scalability, TCC can have multiple servers having the replicas of the trajectories and also the large-scale road network can be divided into multiple regions that have their own TCC for the TSF data forwarding. Each TCC per region performs the reverse data forwarding in the centralized way with the trajectory information. In the performance evaluation in Section 7.7, we will show the impact of multiple APs on the packet delivery delay and the packet delivery ratio, given the user-required delivery probability  $\alpha$ .

## 6.3 Data Forwarding with Multiple Target Points

Up to now we have discussed the data forwarding for a single target point. However, under the light vehicular traffic, the forwarding with a single target point may not provide the reliable data delivery by guaranteeing the user-required data delivery ratio  $\alpha$ . In this case, we can select multiple target points to satisfy  $\alpha$  and send one copy of a packet to each target



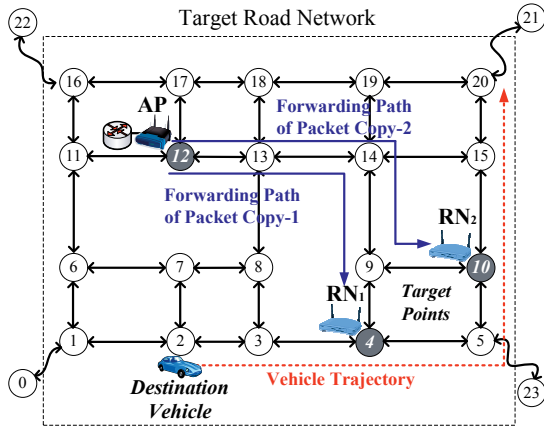


Fig. 7. Data Forwarding with Multiple Target Points

point. In this subsection, we discuss how to select multiple target points for the given  $\alpha$ .

In the multiple target point selection, our objective is to select a minimum number of target points (i.e., a minimum number of packet copies) to satisfy the delivery probability  $\alpha$ . For this objective, the following optimization is used: Let  $I$  be the intersection set on the destination vehicle's trajectory. Let  $f(S)$  be the multi-target-point objective function such that  $f(S) = D(S) + c|S|$  for target point set  $S \in I$  and  $c > 0$  where  $D(S)$  is the average delivery delay for  $S$ . Refer to Appendix B.1 for the detailed derivation of  $D(S)$ . The coefficient  $c$  is set to a positive value such that a small subset  $S_a$  always has a smaller objective function value than a large subset  $S_b$ ; that is,  $f(S_a) < f(S_b)$  for  $|S_a| < |S_b|$ . Refer to Appendix B.2 for the detailed computation of  $c$ ;  $c$  is set to  $E[V_n] - E[V_1]$  (i.e., the difference between the maximum delivery delay and the minimum delivery delay). Thus, the following optimization is used for an optimal target point set  $S^*$ :

$$S^* \leftarrow \arg \min_{S \subset I} f(S) \quad \text{subject to } 1 - \prod_{i \in S} P[P_i > V_i] \geq \alpha. \quad (14)$$

For example, Fig. 7 shows the selection of multiple target points under the delivery probability threshold  $\alpha$ . In this figure, according to (14), intersections  $n_4$  and  $n_{10}$  are target points to minimize the delivery delay with the delivery success probability no less than  $\alpha$ .

In (14), the searching of a minimum set of target points may be costly in terms of computation because the searching considers the possible combinations of target points. For a practical purpose, we can limit the upper bound of the number of target points (as maximum target point number) that can give a reasonable delivery probability for the given threshold  $\alpha$ . In the performance evaluation in Section 7.7, we will show the impact of multiple target points on the delivery performance, given the user-required delivery probability  $\alpha$  and the maximum target point number.

Note that this multiple-target-point data forwarding can be performed in road networks with *multiple APs* through the combination of Equations (13) and (14). This optimization is left as future work.

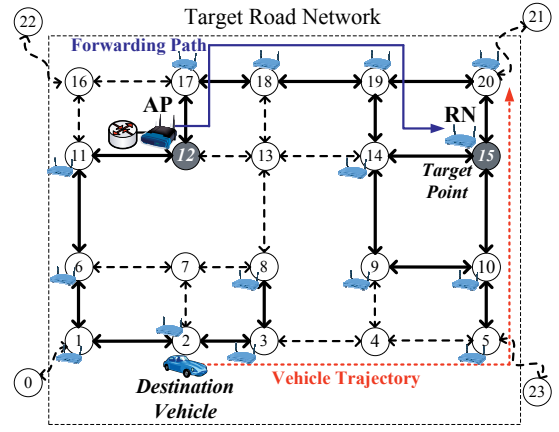


Fig. 8. The Partial Deployment of Relay Nodes

#### 6.4 The Partial Deployment of Relay Nodes

In this subsection, we discuss data forwarding under the partial deployment of relay nodes in the given road network; that is, some intersections might not have their own relay nodes. In this case, we filter out the edges without Relay Node (RN) from the road network graph, as shown in Fig. 8. In the figure, the dotted edges are the filtered ones. With this filtered graph, we can run our target point selection algorithm in Section 4 without any change. Note that the subgraph with the solid edges is used to cover the road network for the reverse data delivery. Clearly, as the number of relay nodes decreases, the data delivery probability from the AP to the destination vehicle will decrease. In the partial deployment of relay nodes, it is important to investigate how to deploy a certain number of relay nodes in order to guarantee the required delivery delay and delivery ratio. This deployment issue is left as future work.

So far we have discussed our TSF protocol considering in realistic settings, such as large-scale road networks. In the following section, we will evaluate our TSF protocol in a variety of road network settings.

## 7 PERFORMANCE EVALUATION

In this section, we evaluate the performance of *TSF*, focusing on our optimal target point selection algorithm. The evaluation setting is as follows:

- **Performance Metrics:** We use (i) *packet delivery delay*, (ii) *packet delivery ratio*, and (iii) *packet delivery cost* (i.e., the number of transmissions) as metrics.
- **Baselines:** Our work is the first attempt for the reverse data forwarding based on the unicast along with the vehicle trajectory, so we have no other state-of-the-art schemes for comparison. To evaluate our target point selection algorithm, we compare the following two target point selection algorithms: (i) Random Trajectory Point (RTP) and (ii) Last Trajectory Point (LTP). In RTP, an intersection is randomly selected among the intersections consisting of the destination vehicle's trajectory. In LTP, the last intersection on the destination vehicle's trajectory is selected as target point. These two baselines might not be best suitable for the performance comparison with

our algorithm, but we use no better existing algorithms available now.

- **Parameters:** We investigate the impacts of the following parameters: (i) *Vehicular traffic density*  $N$ , (ii) *Vehicle speed*  $\mu_v$ , (iii) *Vehicle speed deviation*  $\sigma_v$ , (iv) *Delivery probability threshold*  $\alpha$ , (v) *Access point density*  $M$ , and (vi) *Maximum target point number*  $K$ .

TABLE 3  
Simulation Configuration

Parameter	Description
Road network	The number of intersections is 49. The area of the road map is 8.25km×9km (i.e., 5.1263miles×5.5923miles).
Communication range	$R = 200$ meters (i.e., 656 feet).
Number of vehicles ( $N$ )	The number $N$ of vehicles moving within the road network. The default of $N$ is 250.
Time-To-Live ( $TTL$ )	The expiration time of a packet. The default $TTL$ is the vehicle trajectory's lifetime, that is, the vehicle's travel time for the trajectory, i.e., 2,086 seconds.
Vehicle speed ( $v$ )	$v \sim N(\mu_v, \sigma_v)$ where $\mu_v = \{20, 25, \dots, 60\}$ MPH and $\sigma_v = \{1, 2, \dots, 10\}$ MPH. The maximum and minimum speeds are $\mu_v + 3\sigma_v$ and $\mu_v - 3\sigma_v$ , respectively. The default of $(\mu_v, \sigma_v)$ is (40, 5) MPH.
Vehicle travel path length ( $l$ )	Let $d_{u,v}$ be the shortest path distance from start position $u$ to end position $v$ in the road network. $l \sim N(\mu_l, \sigma_l)$ where $\mu_l = d_{u,v}$ km and $\sigma_l = 3$ km (1.86miles).

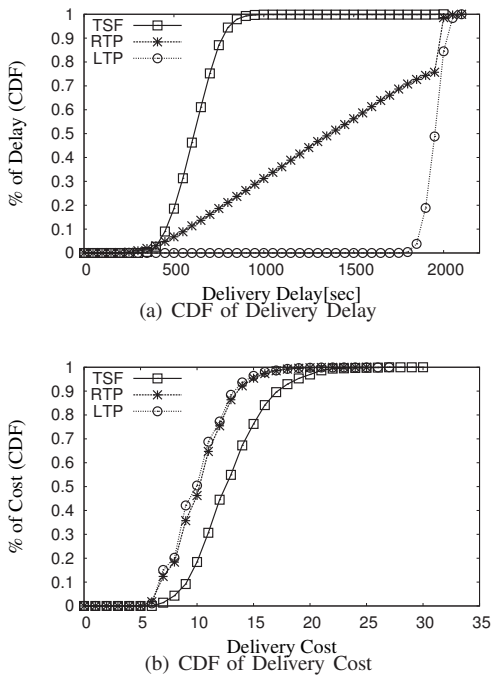


Fig. 9. Cumulative Distributions for Data Delivery

We have built a simulator based on the scheduler provided by SMPL [31] in C with the following settings. A road network with 49 intersections is used in the simulation and one Access Point is deployed in the center of the network. Each vehicle's movement pattern is determined by a *Hybrid Mobility*

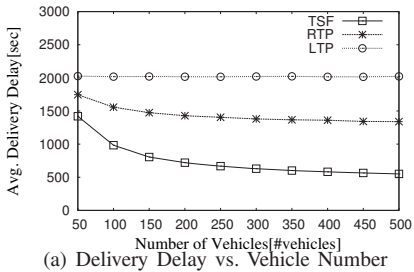
*model* of City Section Mobility model [32] and Manhattan Mobility model [33]. From the characteristics of City Section Mobility, the vehicles are randomly placed at one intersection as *start position* among the intersections on the road network and randomly select another intersection as *end position*. The vehicles move according to the roadways from their start position to their end position. Also, the vehicles wait for a random waiting time (i.e., uniformly distributed from 0 to 10 seconds) at intersections in order to allow the impact of stop sign or traffic signal. From the characteristics of Manhattan Mobility, as shown in Table 3, the vehicle travel path length  $l$  from start position  $u$  to end position  $v$  is selected from a normal distribution  $N(\mu_l, \sigma_l)$  where  $\mu_l$  is the shortest path distance between these two positions and  $\sigma_l$  determines a random detour distance; this random detour distance reflects that all of the vehicles do not necessarily take the shortest path from their start position and their end position. Once the vehicle arrives at its end position, it pauses during a random waiting time and randomly selects another end position. Thus, this vehicle travel process is repeated during the simulation time, based on the hybrid mobility model. On the other hand, among the vehicles, one vehicle is the destination vehicle, circulating in the perimeter of the road network according to its vehicle trajectory during the simulation. The destination vehicle registers its vehicle trajectory into the Traffic Control Center (TCC) in the road network, so the TCC in the simulator knows the accurate trajectory of the destination vehicle all the time.

The vehicle speed is generated from a normal distribution of  $N(\mu_v, \sigma_v)$  [30], as shown in Table 3. The *average vehicle speeds* are used in the vehicle speed distributions to generate vehicle speeds for every two directions per two-way road segment; that is, these two average speeds per road segment can be measured from vehicular traffic by dividing the *road segment length* by the *average travel time* over the road segment. For simplicity, we let all of the road segments have the same speed distribution of  $N(\mu_v, \sigma_v)$  in the road network for the simulation; note that our design can easily extend this simulation setting to having the variety of vehicle speed distributions for road segments.

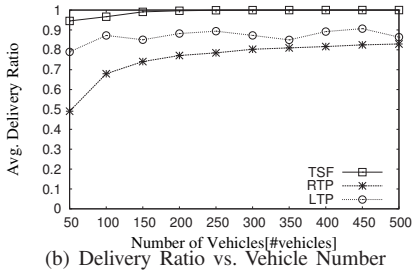
During the simulation, following an exponential distribution with a mean of 5 seconds, packets are dynamically generated from AP in the road network. Note that this data traffic is low because our target application is the delivery of customized road condition information. The total number of generated packets is 2,000 and the simulation is continued until all of these packets are either delivered or dropped due to TTL expiration. The system parameters are selected based on a typical DSRC scenario [8]. Unless otherwise specified, the default values in Table 3 are used.

## 7.1 Forwarding Behavior Comparison

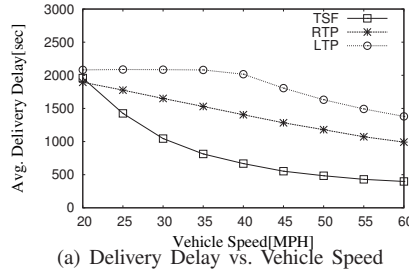
We compare the forwarding behaviors of *TSF*, *RTP* and *LTP* with the cumulative distribution function (CDF) of the packet delivery delay and the packet delivery cost; note that for *TSF*, the delivery probability threshold  $\alpha$  is 95 percent.



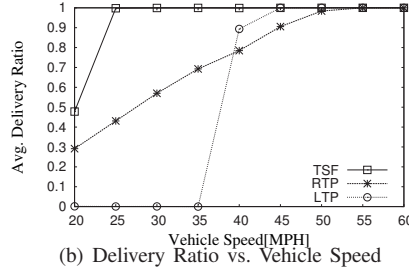
(a) Delivery Delay vs. Vehicle Number



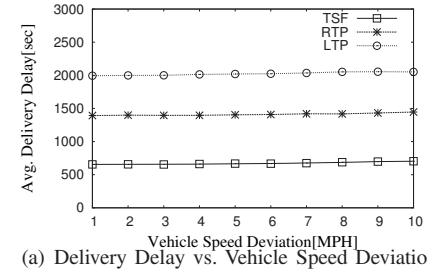
(b) Delivery Ratio vs. Vehicle Number



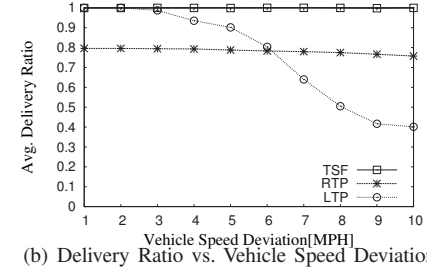
(a) Delivery Delay vs. Vehicle Speed



(b) Delivery Ratio vs. Vehicle Speed



(a) Delivery Delay vs. Vehicle Speed Deviation



(b) Delivery Ratio vs. Vehicle Speed Deviation

Fig. 10. The Impact of Vehicle Number  $N$

Fig. 11. The Impact of Vehicle Speed  $\mu_v$

Fig. 12. The Impact of Vehicle Speed Deviation  $\sigma_v$

First, we analyze the CDF of the packet delivery delay. From Fig. 9(a), it is very clear that *TSF* has much smaller packet delivery delay than *RTP* and *LTP*. For any given packet delivery delay, *TSF* always has a larger CDF value than both of them before they both reach 100-percent CDF. For example, *TSF* reaches 75-percent CDF with a delivery delay of about 745 seconds while the value for *RTP* is about 1,970 seconds and the value for *LTP* is about 2,025 seconds. In other words, on the average packet delivery delay, *TSF* has about 1/2 delay of *RTP* and about 1/3 delay of *LTP*, respectively. Especially, the CDF of *LTP* starts to increase from 1 percent at 1,865 seconds and becomes 99 percent at 2,105 seconds. This CDF is sharply increasing close to the packet TTL (i.e., 2,086 seconds) because the *LTP* chooses the last point on the vehicle trajectory as target point, leading to the long delivery delay.

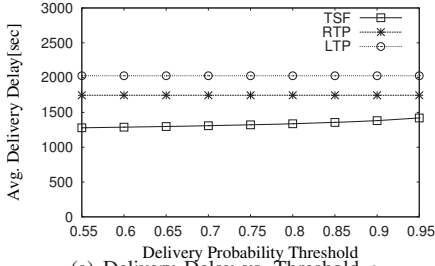
Next, the CDF of the packet delivery cost is analyzed using Fig. 9(b). In this figure, *TSF* has more packet delivery cost at all of the CDF values than the other schemes. This means that *TSF* utilizes the forwarding paths using more packet transmissions than the others. These forwarding paths with more transmissions reduce the carry delay that is the dominant factor of the overall delivery delay, leading to the shorter delivery delay, as discussed for the delivery delay with Fig. 9(a) just before. Note that all of the three schemes (i.e., *TSF*, *RTP* and *LTP*) use relay nodes as temporary packet holders for the reliable data delivery. Clearly, these relay nodes require extra communication overhead for the data forwarding between vehicles and relay nodes. This communication overhead is counted in the packet delivery cost. We will show the performance of the three forwarding schemes quantitatively in the following subsections.

## 7.2 The Impact of Vehicle Number $N$

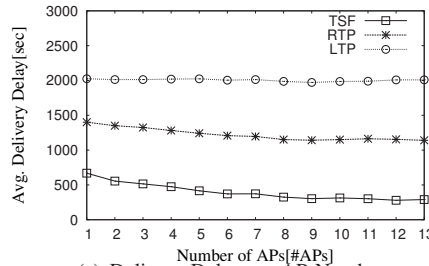
The number of vehicles in the road network determines the vehicular traffic density in a road network. In this subsection,

we intend to study how effectively *TSF* can forward packets from AP toward the destination vehicle using the destination vehicle's trajectory. Through our extensive simulations, we observe that under *any vehicular traffic density*, *TSF* significantly outperforms *RTP* and *LTP* in terms of the packet delivery delay and the packet delivery ratio. Fig. 10(a) shows the packet delivery delay comparison among *TSF*, *RTP* and *LTP* with varying the number of vehicles, that is, from 50 to 500. As shown in Fig. 10(a), *TSF* has much smaller packet delivery delay than *RTP* and *LTP* at all vehicular densities. As expected, one trend is that the delivery delays in *TSF*, *RTP* and *LTP* decrease as the number of vehicles increases. This is because the more vehicles increase the forwarding probability among vehicles, so this reduces the carry delay, leading to the overall shorter delivery delay. The smallest delay reduction of *TSF* is 19 percent at  $N = 50$  for *RTP* and 30 percent at  $N = 50$  for *LTP*, respectively. On the other hand, the largest delay reduction is 59 percent at  $N = 500$  for *RTP* and 73 percent at  $N = 500$  for *LTP*, respectively. From this figure, it can be seen that as the road traffic increases, the trajectory in *TSF* has more contribution to the delivery delay. However, as the traffic density reaches a certain point (e.g.,  $N = 400$ ), the delay of *TSF* does not decrease much. This is because due to the high delivery probability threshold (i.e.,  $\alpha = 95$  percent), *TSF* selects a target point in a conservative way to satisfy the required delivery probability, leading to a small delay improvement.

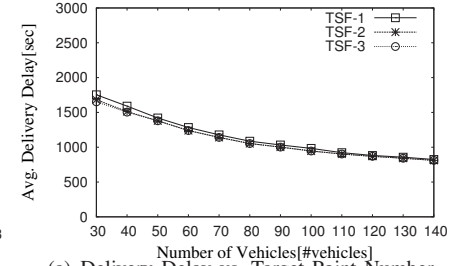
Let us compare the delivery ratios among these three schemes. Fig. 10(b) shows the delivery ratio for the vehicle number. *TSF* has the highest delivery ratio (i.e., about 95 percent) at all the range of the vehicle numbers. One thing to note is that *LTP* does not necessarily have a high delivery ratio (i.e., 87-percent average ratio). As a reminder, *LTP* sends the packet toward the last trajectory point. However, the path from AP to this last point may not be able to deliver the packet to the



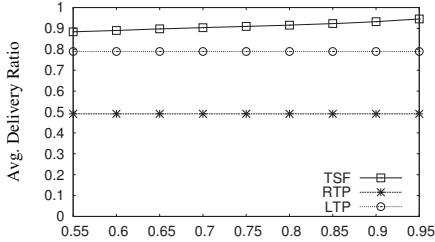
(a) Delivery Delay vs. Threshold  $\alpha$



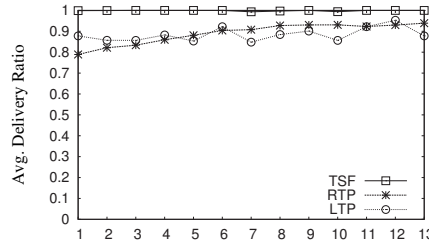
(a) Delivery Delay vs. AP Number



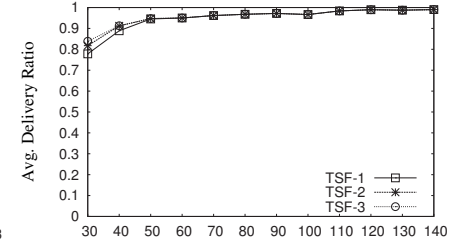
(a) Delivery Delay vs. Target Point Number



(b) Delivery Ratio vs. Threshold  $\alpha$



(b) Delivery Ratio vs. AP Number



(b) Delivery Ratio vs. Target Point Number

Fig. 13. The Impact of Delivery Probability Threshold  $\alpha$

Fig. 14. The Impact of AP Number  $M$

Fig. 15. The Impact of Maximum Target Point Number  $K$

last point before the destination vehicle arrives at the last point. This is because the path to the target point is selected without considering the delivery probability, so the packet delivery delay to the target point can be longer than the destination vehicle's travel delay. Therefore, with the optimal target point, *TSF* has better performance than *RTP* and *LTP* in terms of two performance metrics. This indicates the importance of an optimal target point selection for the data delivery.

### 7.3 The Impact of Vehicle Speed $\mu_v$

In this subsection, we investigate how the change of mean vehicle speed affects the delivery delay. Fig. 11(a) shows the delivery delay under different mean vehicle speeds. As shown in the Fig. 11(a), for *TSF*, *RTP* and *LTP*, the higher vehicle speed leads to the shorter delivery delay. This is because the high vehicle speed yields high vehicle arrival rate at each road segment, leading to the shorter delivery delay. However, at all vehicle speeds, the *TSF* still outperforms both *RTP* and *LTP*. For the delivery ratio, as shown in Fig. 11(b), the *TSF* has much better performance than the others.

### 7.4 The Impact of Vehicle Speed Deviation $\sigma_v$

In this subsection, we investigate the impact of vehicle speed deviation on the performance. We found that under a variety of vehicle speed deviations, *TSF* provides a shorter delay and a more reliable data delivery than both *RTP* and *LTP*. Fig. 12(a) illustrates our observation for the delivery delay according to the vehicle speed deviation when the number of vehicles is  $N = 250$ . The delay performance gaps among these three schemes are almost constant at all of the vehicle speed deviations from 1 MPH to 10 MPH. However, for the delivery ratio, as shown in Fig. 12(b), *TSF* provides a reliable delivery close to 100 percent, however the others have worse

performance. Especially, *LTP*'s delivery ratio degrades sharply as the vehicle speed deviation increases. This is because under a higher speed deviation, *LTP* can provide less timely delivery to the target point. On the other hand, *TSF* supports the timely delivery to the target point with the delivery probability considering this speed deviation.

### 7.5 The Impact of Delivery Probability Threshold $\alpha$

In this subsection, we investigate the impact of the user-required delivery probability threshold  $\alpha$  on both the delivery delay and the delivery ratio. For this investigation, we run three schemes under a light-traffic road network where the number of vehicles is  $N = 50$ .

Fig. 13(a) and Fig. 13(b) show the delivery delay and the delivery ratio according to  $\alpha$ , respectively. First of all, *RTP* and *LTP* are not affected by the threshold  $\alpha$  because they do not consider the delivery probability in their target point selection. In the delivery delay, as shown in Fig. 13(a), *TSF*'s delivery delay increases slightly as  $\alpha$  increases. This is because for a higher  $\alpha$ , *TSF* selects a target point in a more conservative way such that the packet will arrive at the target point earlier than the destination vehicle with a higher probability, so the actual delivery to the destination vehicle can be longer. This conservative way leads to the higher delivery ratio as  $\alpha$  increases, as shown in Fig. 13(b). Therefore, there exists a trade-off between the delivery delay and the delivery ratio according to  $\alpha$ . For example, in the interval from  $\alpha = 0.85$  to  $\alpha = 0.95$  in Fig. 13, the delivery ratio is getting better, but the delivery delay is getting worse.

### 7.6 The Impact of AP Number $M$

In this subsection, we explain how multiple Access Points (APs) have an impact on the performance. Note that multiple

APs are uniformly placed in the road network in the simulation. The other parameters are set to the default values in Table 3; that is, the number of vehicles is  $N = 250$ . In this multiple-AP setting, we need to select an appropriate AP among the set of APs. *TSF* selects an AP with the minimum vehicle delay to the target point satisfying the required delivery probability, as discussed in Section 6.2. Both *RTP* and *LTP* select an AP with the minimum packet delay to the target point.

As shown in Fig. 14(a), the delivery delay in both *TSF* and *RTP* decreases as the AP number increases; this is because they select an AP to provide a shorter delivery delay. However, *LTP*'s delay is almost constant regardless of the increase of the AP number; this is because *LTP* selects the last trajectory point as target point, so the packets have to wait for the packet destination at the target points until the destination vehicle arrives at the target point. Actually, the vehicle travel time to this target point will decide the actual delivery delay. As seen from Fig. 14(a), in order to achieve a shorter delivery delay, we need to deploy more APs to cover the target road network. For example, with one AP, *TSF* can provide the average delivery delay of 669 seconds, but with 13 APs, it can provide the average delivery delay of 290 seconds, that is, only 43 percent of the delivery delay in one AP.

For the delivery ratio, as shown in Fig. 14(b), *TSF* has a high ratio of at least 99 percent in all of the cases. Note that the required delivery probability  $\alpha$  is 95 percent and the actual data delivery ratio satisfies this required threshold  $\alpha$ . For the delivery cost, we observed that all of the three schemes tend to have a less number of transmissions as the number of APs increases. This is because with a more number of APs, each AP needs to cover a smaller road network area for the data delivery. For example, *TSF* needs 13 transmissions with 1 AP, but it needs only 5 transmissions with 13 APs.

Therefore, with more APs, we can reduce the delivery delay while guaranteeing the data delivery ratio  $\alpha$ . How to deploy how many APs into a road network is left as future work in order to satisfy the user-required delivery delay and delivery ratio along with the deployment of relay nodes at intersections and in the middle of road segments in the target road network.

### 7.7 The Impact of Maximum Target Point Number $K$

In light vehicular traffic road networks, the single packet for a single target point may not satisfy the user-required delivery probability  $\alpha$ , as discussed in Section 6.3. In this case, as one method, we can increase the number of target points such that one copy of a packet is sent to each target point. In this subsection, we show the impact of multiple target points in *TSF*.

Fig. 15 shows the packet delivery delay and the packet delivery ratio according to the vehicular traffic density, that is, from 30 vehicles to 140 vehicles. *TSF* has three versions for maximum target point number: (a) *TSF* with 1 target point (TSF-1), (a) *TSF* with 2 target points (TSF-2), and (a) *TSF* with 3 target points (TSF-3). In the optimization of (14) in Section 6.3, the maximum target point number limits the number of target points satisfying the user-required delivery probability ( $\alpha = 95$  percent) *either* exactly *or* as much as

possible. That is, when the target points for the maximum target point number  $K$  cannot satisfy  $\alpha$ , the AP chooses  $K$  target points with the maximum delivery probability (computed in the optimization in (14)) and then sends the packet copies of the corresponding number  $K$  toward the target points. On the other hand, under the maximum target point number of  $K$ , when a single packet copy with a single target point can satisfy  $\alpha$ , only one packet will be sent toward the corresponding target point.

As shown in Fig. 15(a) and Fig. 15(b), in extremely light vehicular networks (e.g., 30 or 40 vehicles), the greater maximum target point number leads to the better performance, that is, the shorter delivery delay and the higher delivery ratio. Once the vehicular traffic density reaches a certain point (i.e., 120 vehicles), TSF-1, TSF-2, and TSF-3 have almost the same performance because in most cases, a single target point can satisfy the user-required delivery probability in the optimization in (14) in Section 6.3. Thus, it can be seen that under not-extremely-light vehicular density, a single-target-point data forwarding (i.e., TSF-1) is enough to deliver data packets to a destination vehicle, satisfying the user-required delivery probability  $\alpha$ .

For the delivery cost, we observed that the data forwarding with a more maximum target points has a higher cost because the number of target points determines the number of packet copies. All of the three schemes become to have the same cost (i.e., 12 transmissions) once the number of vehicles is at least 50. This is because after a certain of vehicle density, the required number of target points is fixed to guarantee the given delivery probability  $\alpha$ .

## 8 CONCLUSION

In this paper, we propose a Trajectory-based Statistical Forwarding (TSF) in vehicular networks, where the carry delay is the dominating factor for the End-to-End delivery delay. Our goal is to provide a reliable, efficient infrastructure-to-vehicle data delivery by minimizing the packet delivery delay subject to the required delivery probability. This goal is achieved by computing an optimal target point as *packet-and-vehicle-rendezvous-point* with the vehicle delay distribution and the packet delay distribution, which can be obtained from the vehicle trajectory and the vehicular traffic statistics, respectively. Once an optimal target point is determined, through the shortest-delivery-delay path from the Access Point to the mobile destination, packets are source-routed toward the packet destination. As future work, we will investigate how to deploy infrastructure nodes for the user-required performance with the minimum deployment cost and also how to fully utilize the trajectories of vehicles used as packet forwarders or carriers for the more efficient data forwarding in vehicular networks.

## ACKNOWLEDGMENT

This research is supported in part by NSF grants CNS-0917097/0845994/0720465 and 1016350/0960833, by MSI and DTC at the University of Minnesota, and by the grant of Singapore-MIT IDC IDD61000102.

## REFERENCES

- [1] V. Naumov and T. R. Gross, "Connectivity-Aware Routing (CAR) in Vehicular Ad Hoc Networks," in *INFOCOM*. IEEE, May 2007.
- [2] Q. Xu, R. Sengupta, and D. Jiang, "Design and Analysis of Highway Safety Communication Protocol in 5.9 GHz Dedicated Short Range Communication Spectrum," in *VTC*. IEEE, Apr. 2003.
- [3] J. Zhao and G. Cao, "VADD: Vehicle-Assisted Data Delivery in Vehicular Ad Hoc Networks," *IEEE Transactions on Vehicular Technology*, vol. 57, no. 3, pp. 1910–1922, May 2008.
- [4] A. Skordylis and N. Trigoni, "Delay-bounded Routing in Vehicular Ad-hoc Networks," in *MOBIHOC*. ACM, May 2008.
- [5] J. Ott and D. Kutscher, "Drive-thru Internet: IEEE 802.11b For "Automobile" Users," in *INFOCOM*. IEEE, Mar. 2004.
- [6] J. Eriksson, H. Balakrishnan, and S. Madden, "Cabernet: Vehicular Content Delivery Using WiFi," in *MOBICOM*. ACM, Sep. 2008.
- [7] V. Bychkovsky, B. Hull, A. Miu, H. Balakrishnan, and S. Madden, "A Measurement Study of Vehicular Internet Access Using In Situ Wi-Fi Networks," in *MOBICOM*. ACM, Sep. 2006.
- [8] A. Carter, "The Status of Vehicle-to-Vehicle Communication as a Means of Improving Crash Prevention Performance," Tech. Rep. 05-0264, 2005, <http://www-nrd.nhtsa.dot.gov/pdf/nrd-01/esv/esv19/05-0264-W.pdf>.
- [9] H. Yomogita, "Mobile GPS Accelerates Chip Development," <http://techon.nikkeibp.co.jp/article/HONSHI/20070424/131605/>.
- [10] Philadelphia Department of Transportation, "Traffic Control Center," <http://philadelphia.pahighways.com/philadelphiatcc.html>.
- [11] Hawaii Department of Transportation, "Traffic Information Center," <http://www.eng.hawaii.edu/Trafficam/waikiki.html>.
- [12] ETSI, "DSRC Standardization," <http://www.etsi.org/WebSite/Technologies/DSRC.aspx>.
- [13] Toyota Motor Corporation (TMC), "TMC Develops Onboard DSRC Unit to Improve Traffic Safety," <http://www2.toyota.co.jp/en/news/09/09/0903.html>.
- [14] J. Burgess, B. Gallagher, D. Jensen, and B. N. Levine, "MaxProp: Routing for Vehicle-Based Disruption-Tolerant Networks," in *INFOCOM*. IEEE, Apr. 2006.
- [15] A. Vahdat and D. Becker, "Epidemic Routing for Partially-connected Ad Hoc Networks," Tech. Rep., 2000, <http://www.cs.duke.edu/~vahdat/ps/epidemic.pdf>.
- [16] J. Jeong, S. Guo, Y. Gu, T. He, and D. Du, "Trajectory-Based Data Forwarding for Light-Traffic Vehicular Ad-Hoc Networks," *IEEE Transactions on Parallel and Distributed Systems*, vol. 22, no. 5, pp. 743–757, May 2011.
- [17] Y. Ding, C. Wang, and L. Xiao, "A Static-Node Assisted Adaptive Routing Protocol in Vehicular Networks," in *VANET*. ACM, Sep. 2007.
- [18] L. Pelusi, A. Passarella, and M. Conti, "Opportunistic Networking: Data Forwarding in Disconnected Mobile Ad Hoc Networks," *IEEE Communications Magazine*, vol. 44, no. 11, pp. 134–141, Nov. 2006.
- [19] Garmin Ltd., "Garmin Traffic," <http://www8.garmin.com/traffic/>.
- [20] H. Wu, R. Fujimoto, R. Guensler, and M. Hunter, "MDDV: A Mobility-Centric Data Dissemination Algorithm for Vehicular Networks," in *VANET*. ACM, Oct. 2004.
- [21] P. Rodriguez, R. Chakravorty, J. Chesterfield, I. Pratt, and S. Banerjee, "MAR: A Commuter Router Infrastructure for the Mobile Internet," in *MOBISYS*. ACM, Jun. 2004.
- [22] E. M. Royer and C.-K. Toh, "A Review of Current Routing Protocols for Ad-hoc Mobile Wireless Networks," *IEEE Personal Communications*, vol. 6, no. 2, pp. 46–55, Apr. 1999.
- [23] N. Wisitpongphan, F. Bai, P. Mudalige, and O. K. Tonguz, "On the Routing Problem in Disconnected Vehicular Ad Hoc Networks," in *INFOCOM Mini-symposia*. IEEE, May 2007.
- [24] N. Banerjee, M. D. Corner, D. Towsley, and B. N. Levine, "Relays, Base Stations, and Meshes: Enhancing Mobile Networks with Infrastructure," in *MOBICOM*. ACM, Sep. 2008.
- [25] Jupiter Research, "Municipal Wireless: Partner to Spread Risks and Costs While Maximizing Benefit Opportunities," Tech. Rep., Jun. 2005.
- [26] General Motors (GM), "Vehicle-to-Vehicle (V2V) Communications," <http://www.gm.com/experience/technology/research/overview/isl/vcim.jsp>.
- [27] Savari Networks, "StreetWAVE: Roadside Unit," <http://www.savarinetworks.com/files/StreetWAVE-DS-final.pdf>.
- [28] M. DeGroot and M. Schervish, *Probability and Statistics (3rd Edition)*. Addison-Wesley, 2001.
- [29] A. Polus, "A Study of Travel Time and Reliability on Arterial Routes," *Transportation*, vol. 8, no. 2, pp. 141–151, Jun. 1979.
- [30] D. S. Berry and D. M. Belmont, "Distribution of Vehicle Speeds and Travel Times," in *Proceedings of the Second Berkeley Symposium on Mathematical Statistics and Probability*, Jul. 1950.
- [31] M. MacDougall, *Simulating Computer Systems: Techniques and Tools*. MIT Press, 1987.
- [32] T. Camp, J. Boleng, and V. Davies, "A Survey of Mobility Models for Ad Hoc Network Research," *Wireless Communications and Mobility Computing (WCMC): Special Issue on Mobile Ad Hoc Networking: Research, Trends and Applications*, vol. 2, pp. 483–502, Aug. 2002.
- [33] F. Bai, N. Sadagopan, and A. Helmy, "IMPORTANT: A framework to systematically analyze the Impact of Mobility on Performance of Routing protocols for Adhoc Networks," in *INFOCOM*. IEEE, Mar. 2003.



**Jaehoon (Paul) Jeong** is a software engineer in Brocade Communications. He received the Ph.D. degree under Professor David H.C. Du and Professor Tian He from the Department of Computer Science and Engineering at the University of Minnesota in 2009. He received the B.S. degree from the Department of Information Engineering at Sungkyunkwan University in Korea and the M.S. degree from the School of Computer Science and Engineering at Seoul National University in Korea, in 1999 and 2001, respectively.



**Shuo Guo** received her B.S. in Electronic Engineering at Tsinghua University in 2006 and is currently a Ph.D. candidate in the Department of Electrical and Computer Engineering at the University of Minnesota, Twin Cities. Her research includes Wireless Sensor Networks, Vehicular Ad-Hoc Networks, and Real-time and Embedded Systems. She received a best paper award at IEEE MASS 2008.



**Yu (Jason) Gu** is an assistant professor at the Singapore University of Technology and Design. He received the Ph.D. degree in the Department of Computer Science and Engineering at the University of Minnesota, 2010. He is the author and co-author of over 21 papers in premier journals and conferences. His publications have been selected as graduate-level course materials by over 10 universities in the United States and other countries. He has received several prestigious awards from the University of Minnesota.



**Tian He** is currently an associate professor in the Department of Computer Science and Engineering at the University of Minnesota-Twin City. He received the Ph.D. degree under Professor John A. Stankovic from the University of Virginia, Virginia in 2004. Dr. He is the author and co-author of over 90 papers in premier sensor network journals and conferences with over 4000 citations. His publications have been selected as graduate-level course materials by over 50 universities in the United States and other countries.



**David H.C. Du** received the B.S. degree in mathematics from National Tsing-Hua University, Taiwan, R.O.C. in 1974, and the M.S. and Ph.D. degrees in computer science from the University of Washington, Seattle, in 1980 and 1981, respectively. He is currently the Qwest Chair Professor at the Computer Science and Engineering Department, University of Minnesota, Minneapolis. His research interests include cyber security, sensor networks, multimedia computing, storage systems, and high-speed networking.